



Dissolved organic phosphorus enhances arsenate bioaccumulation and biotransformation in *Microcystis aeruginosa*[☆]

Zhenhong Wang^{a, b, d, **, *}, Herong Gui^b, Zhuaxi Luo^{c, d, *, *}, Zhuo Zhen^c, Changzhou Yan^c, Baoshan Xing^d

^a College of Chemistry and Environment, Fujian Province Key Laboratory of Modern Analytical Science and Separation Technology, Minnan Normal University, Zhangzhou 363000, China

^b National Engineering Research Center of Coal Mine Water Hazard Controlling (Suzhou University), Suzhou, Anhui, 234000, China

^c Key Laboratory of Urban Environment and Health, Institute of Urban Environment, Chinese Academy of Sciences, Xiamen 361021, China

^d Stockbridge School of Agriculture, University of Massachusetts, Amherst, MA 01003, USA

ARTICLE INFO

Article history:

Received 1 April 2019

Received in revised form

29 June 2019

Accepted 29 June 2019

Available online 3 July 2019

Keywords:

Arsenate

Subcellular distribution

Functional gene

Organic phosphorus

Algae

ABSTRACT

Only limited information is available on the effects of dissolved organic phosphorus (DOP) on arsenate (As(V)) bioaccumulation and biotransformation in organisms. In this study, we examined the influence of three different DOP forms (β -sodium glycerophosphate (β P), adenosine 5'-triphosphate (ATP), and D-Glucose-6-phosphate disodium (GP) salts) and inorganic phosphate (IP) on As(V) toxicity, accumulation, and biotransformation in *Microcystis aeruginosa*. Results showed that *M. aeruginosa* utilized the three DOP forms to sustain its growth. At a subcellular level, the higher phosphorus (P) distribution in metal-sensitive fractions (MSF) observed in the IP treatments could explain the comparatively lower toxic stress of algae compared to the DOP treatments. Meanwhile, the higher MSF distribution of arsenic (As) in *M. aeruginosa* in the presence of DOP could explain the higher toxicity with lower 96-h half maximal effective concentration (EC₅₀) values. Although we observed As(V) and P discrimination in *M. aeruginosa* under IP treatments with high intracellular P/As, we did not find this discrimination under the DOP treatments. As accumulation in algal cells was therefore greatly enhanced by DOP, especially β P, given its lower transformation rate to phosphate compared to ATP and GP in media. Additionally, As(V) reduction and, subsequently, As(III) methylation were greatly facilitated in *M. aeruginosa* by the presence of DOP, particularly GP, which was confirmed by the higher relative expression of its two functional genes (*arsC* and *arsM*). Our findings indicate that As(V) accumulation and its subsequent biotransformation were enhanced by organic P forms, which provides new insight into how DOP modulates As metabolism in algae.

© 2019 Elsevier Ltd. All rights reserved.

1. Introduction

Phosphorus (P), being a key chemical element that restricts growth in many eutrophic freshwater (Hudson et al., 2000) and marine environments (Wu et al., 2000), can enhance the

proliferation of undesirable organisms that respond to ecological dominance (Haygarth et al., 2005). In water, P is often partitioned into organic P and its inorganic orthophosphate forms. Organic P further exists in nucleic acids, phosphoproteins and amino phosphoric acids, phospholipids, phytic acid, phosphonates, riboflavin monophosphate, and organic condensed P compounds, such as adenosine triphosphate. Additionally, organic P can be at least as abundant as inorganic P in certain freshwater systems (Karl and Björkman, 2001; Worsfold et al., 2016) while also acting as a P source for some algae and cyanobacteria to support primary production (Bengt Bostriim and Broberg, 1988; Huang et al., 2005; Hudson et al., 2000; Qin et al., 2015). Dissolved organic phosphorus (DOP) can derive from the degradation of glycolipids, glycoproteins, and antibiotics, which can exceed concentrations of dissolved inorganic phosphate (IP) in certain water bodies, and varies both

[☆] This Paper has been recommended for acceptance by Dr. Jörg Rinklebe

* Corresponding author. Key Laboratory of Urban Environment and Health, Institute of Urban Environment, Chinese Academy of Sciences, Xiamen 361021, China.

** Corresponding author. College of Chemistry and Environment, Fujian Province Key Laboratory of Modern Analytical Science and Separation Technology, Minnan Normal University, Zhangzhou 363000, China.

E-mail addresses: zhhwang1979@163.com (Z. Wang), zxluoie@163.com (Z. Luo).

temporally and spatially within the range of 1.1–22 µg/L (Li et al., 2015; Phil Monbet and Worsfold, 2009). Furthermore, DOP forms, such as adenosine 5'-triphosphate (ATP), adenosine monophosphate, and glucose-6-phosphate (GP), can readily be converted to orthophosphate forms, making them directly accessible for aquatic microbial bioavailability (Björkman and Karl, 2003; Li and Brett, 2013). At the same time, *Microcystis* could exploit DOP sources to form blooms by excreting phosphatases (Whitton et al., 1991) within high DOP-dominated lakes at low inorganic P levels (Harke et al., 2012; Wang et al., 2017a). Therefore, DOP represents a major P reservoir within certain surface water bodies (Monbet et al., 2007).

Arsenic (As), a major toxic and carcinogenic substance, has caused concern due to its pervasiveness and potential threats to the environment (Hughes et al., 2011; Rahman et al., 2014). In environments, As can exist in inorganic forms (i.e., arsenite (As(III)) and arsenate (As(V))) and organic forms (i.e., monomethylarsonic acid (MMA), dimethylarsinic acid (DMA), etc.) (Mandal and Suzuki, 2002). As(V) is the most abundant form of As in oxidized environments (Oremland and Stolz, 2003). Over the last several decades, the effects and mechanisms of IP on As(V) metabolism in microorganisms (Chen et al., 2016; Davis et al., 2015; Elias et al., 2012; Markley and Herbert, 2010; Miao et al., 2012; Wang et al., 2016; Zhang et al., 2014) and plants (Lei et al., 2012; Lessl and Ma, 2013; Panuccio et al., 2012; Secco et al., 2013) have been extensively investigated and tentatively discussed. Due to the similar chemical structure of As(V) and IP, As(V) toxicity and its bioaccumulation and biotransformation in organisms are impacted by different levels of IP in the environment, thus affecting As biogeochemical cycling and its potential for bioremediation (Levy et al., 2005; Wang et al., 2016; Wang et al., 2014). To date, only a limited number of studies pertaining to the effects of DOP on As(V) metabolism in organisms have been published.

Furthermore, there remains widespread concern on the important role that microalgae play in As metabolization, including its accumulation and transformation in environments through potential algal bioremediation under As contamination and its corresponding transfer risks into the food chain (Rahman et al., 2012; Wang et al., 2018). As mentioned above, DOP can be advantageously used by certain algae in aquatic ecosystems. In turn, the different utilization modes of DOP (compared to IP) in algal cells can undeniably influence As metabolism in algae. To understand the extent as well as the way in which DOP impacts As(V) metabolism in algae, we selected three DOP species, namely, β-sodium glycerophosphate (βP), adenosine 5'-triphosphate (ATP), and beta-D-glucose-6-phosphate (GP), and IP to investigate the status of algal growth, As uptake and biotransformation, intracellular As, and P accumulation, including their specific subcellular distribution in algal cells as well as the relevant gene expression function of As and P metabolism in algae. *Microcystis aeruginosa* (*M. aeruginosa*) is recognized for its ability to accumulate high levels of As in freshwater, thereby providing greater potential for As bioremediation and biogeochemical cycling in freshwater systems (Kaneko et al., 2007; Wang et al., 2018; Wang et al., 2017b). Accordingly, *M. aeruginosa* was selected as the algal model organism. The obtained results could provide new insight into how DOP modulates As metabolism in algae, thereby increasing our understanding of As biogeochemical cycling in freshwater ecosystems as well as its potential for algal bioremediation in As contaminated water bodies.

2. Materials and methods

2.1. Algal culture and preparation

Stock solutions were prepared for the three different DOP forms

(βP, ATP, and GP) and IP (KH₂PO₄) with 100.0 mg P/L. Meanwhile, modified BG11 media were prepared at 5.0 mg P/L for the 7-d algal growth and 96 h As(V) toxicity experiments, and at 1.0 mg P/L for the 10 d As(V) metabolism experiments. The As(V) solution was prepared using Na₃AsO₄·12H₂O (Fluka, p.a.). Specifically, IP was considered as the control group in the following experiments since the results obtained between DOP and IP were compared in this study.

M. aeruginosa FACHB-905 specimens were obtained from the Institute of Hydrobiology, Chinese Academy of Sciences, China. Prior to the experiments, microalgae were preserved and grown in a sterile BG11 media without the addition of phosphate for 48 h until it reached a condition of P deficiency. Afterwards the microalgae were cultured in BG11 media using the different modified P sources from which to conduct the experiments. The culture conditions used in our experiments have been previously described in detail (Wang et al., 2017b).

2.2. Algal growth and toxic effects of arsenate

Specimens of *M. aeruginosa* were aseptically transferred to the modified BG11 media imbued with different P sources (i.e., IP, βP, ATP, and GP) after twice washing in sterile deionized water (DI water). To confirm whether algae could adequately grow solely under P conditions (i.e., without the addition of As), the algae specimens were cultured in an illuminated incubator shaker for 7 d. The optical density (OD) of algal cells at 680 nm, chlorophyll *a* (Chl *a*), and the maximum photosynthetic quantum yield of PSII (yield) were determined daily to describe algal growth characteristics. Following this, we conducted the 96 h toxicity tests of As(V) with *M. aeruginosa* under the different P treatments (IP, βP, ATP, and GP) to determine the 96-h half maximal effective concentration (EC₅₀) values (concentrations corresponding to 50% inhibition effects) of OD, Chl *a*, and yield, which were calculated by fitting them with a sigmoidal dose-response curve equation (Karadjova et al., 2008). Specifically, As(V) treatments ranged from 2 to 2.0 × 10⁶ µg/L in the modified media. Thereafter, OD, Chl *a*, and yield were also determined every 24 h.

2.3. Uptake and biotransformation of arsenic and phosphorus

To investigate whether differences in As(V) metabolism occurred in *M. aeruginosa* under the different P treatments (IP, βP, ATP, and GP), algae specimens (with a final total volume of 100 mL) were exposed to 100 µg/L As(V) in the modified BG11 media imbued with the different P sources (i.e., IP, βP, ATP, and GP) for 10 d. According to previous methods used for sample preparation and As analysis (Wang et al., 2018; Wang et al., 2014), we measured As species in algal cells and media, the total arsenic (TAs) and total phosphorus (TP) that accumulated in algae as well as their distribution at a subcellular level, and TP and IP changes observed in media at the conclusion of the experiment.

Furthermore, the subcellular distribution experiments were conducted according to the differential centrifugation procedure (Li et al., 2011; Li et al., 2016). Five fractions were acquired, namely, cellular debris (Debris; containing cell membranes), organelle-containing fraction (Organelles; i.e., chloroplasts, mitochondria, and lysosome), heat-denatured proteins (HDP; containing enzymes), heat-stable proteins (HSP; metallothionein-like proteins), and metal-rich granules (MRG). Additionally, TAs and TP were determined for the five fractions.

Moreover, in order to understand to what extent DOP changes into IP in the algal solution, the transformation of the selected DOP forms into IP was investigated by measuring IP daily in the ensuing extracellular secretion media collected. To obtain the extracellular

secretion media, *M. aeruginosa* specimens were cultured as per the aforementioned condition in P-free BG11 for 3 d, then centrifuged at 4000 rpm for 15 min in order to collect the supernatant. Afterwards, the three DOP forms with an initial P concentration of 1 mg/L were added to the extracellular secretion media we obtained (i.e., the aforementioned supernatant), and then we measured IP levels daily for 6 d. Furthermore, the IP transformation rates for the three DOP forms in the algal solution were assessed using a linear kinetic model. All above treatments were generated in triplicate with a re-suspended initial cell density of approximately 10^6 cells/mL.

2.4. Chemical analysis

The samples we obtained as per the above procedures were further diluted to measure As using inductively coupled plasma mass spectrometry (ICP-MS) and As speciation using high-performance liquid chromatography coupled to inductively coupled plasma-mass spectrometry (HPLC-ICP-MS) (i.e., Agilent LC1100 series coupled with the Agilent ICP-MS 7500a) (Wang et al., 2018; Wang et al., 2014). Additionally, TP and IP concentrations were measured using the modified molybdenum-antimony spectrophotometric method, which utilized L-cysteine to eliminate As(V) interference (Xu et al., 2014). Chl *a* and yield were measured using a Phyto-PAM-fluorometer (Phyto-PAM, Walz, Germany) (Chalifour and Juneau, 2011).

2.5. Isolation of RNA and Real-Time PCR functional gene expressions

The TRIzol reagent (Life Technology, Beijing, China) was used to isolate total RNA from *M. aeruginosa* under the different P treatments. Traces of DNA were removed by incubation with DNase-I (Ambion). The OD₂₆₀/OD₂₈₀ of the RNA obtained ranged from 1.75 to 1.90. The RNA was dissolved in RNase-free water and stored at -80°C . Utilizing the Transcriptor First Strand cDNA Synthesis Kit (Roche), it was determined that the reverse transcription reaction mixtures contained 2 μL of dNPT, 1 μL of Oligo (dT)₁₈ primers, and 13 μL of total RNA. The mixtures were heated at 65°C for 10 min and rapidly cooled down on ice. Following this step, we added 4 μL of a 5×2 buffer, 2 μL of M-mlv, and 40 units of RNasin (an RNase inhibitor) for a total volume of 20 μL after cooling. The mixture was incubated at 25°C for 10 min and at 55°C for 50 min and then heated to 85°C for 5 min to inactivate the reverse transcription reaction.

Four functional genes were selected, including *arsM* (SAM-dependent methyltransferase), *arsC* (arsenate reductase), and NIES-843-1 and NIES-843-2 (5862636: phosphate ABC transporter ATP-binding protein; 5866103: phosphate transport system regulatory protein), which associate with As and P behavior in *M. aeruginosa* (Table S1). The 16S rRNA gene was the reference gene used. Primers were designed using NCBI Primer-Blast (Table S1). The SYBR GREEN PCR kit (Takara) was used for Real-Time PCR, which was conducted using the CFX-96 Touch realtime quantitative polymerase chain reaction system (BIO-RAD, USA). The thermal cycle setting was as follows: 2 min at 95°C , 40 cycles of 15 s at 95°C , 20 s at 58°C , 20 s at 72°C , and 2 min at 72°C . The BIO-RAD version 10 software package was used for sample analysis. We sequenced Real-Time PCR products and conducted sequence alignments to verify product specificity.

2.6. Statistical analysis

Data were recorded as means with their corresponding standard deviations (SD). Bivariate analysis was conducted using IBM SPSS Statistics 23 to determine the correlations between yield and OD and Chl *a*. One-way analysis of variance (ANOVA) was used to

determine the differences between the resultant data among the different P treatments. Significant differences were considered acceptable when $P < 0.05$. Graphics were generated using Origin Pro 2017.

3. Results and discussion

3.1. Algal growth

M. aeruginosa was found to be capable of using all four P forms (i.e., IP, βP , ATP, and GP) as the sole P source by which to maintain algal cell proliferation and growth (Fig. S1). Similarly, some studies also reported that *M. aeruginosa*, *Synechococcus*, and *Trichodesmium* were capable of using βP , ATP, and GP as the sole P source to promote growth (Fu et al., 2006; Li et al., 2015; Orchard et al., 2010; Ren et al., 2017). Specifically, both OD and Chl *a* increased linearly over time under the different P treatments. Additionally, OD differences were not significant under βP and ATP ($P > 0.1$), but significant under IP and GP ($P < 0.05$), indicating that GP had a significant impact on the cell number of algae. For Chl *a*, significant differences were observed under βP and ATP treatments but not under IP and GP treatments. The biosynthesis of Chl *a* in algae was more effective under the βP and ATP treatments than under the IP and GP treatments (Fig. S1b). Similarly, *Synechococcus* CCMP 1334 was also found to exhibit more rapid P assimilation under the ATP treatment than under the IP treatment when algal cells were grown in IP-limited cultures (Fu et al., 2006).

Additionally, significant differences ($P < 0.05$) were found in yield with a linear decreasing trend under the DOP (i.e., βP , ATP, and GP) treatments compared to the IP treatment (Fig. S1c). Furthermore, under DOP treatments, yield values were relatively stable and showed no significant differences ($P > 0.1$; Fig. S1c). Compared to IP, lower yields observed under the DOP treatments (Fig. S1c) indicated that DOP as the sole algal P source was not conducive to the transformation of photoenergy. Comparable to a previous study (Lippemeier et al., 2003), the deficiency or limitation of P as a photosynthetic substrate of algae could decrease the quantum yield of photosynthetic electron transport. Moreover, both OD and Chl *a* were negatively correlated to yield under the different P treatments (Table 1). These negative correlations implied that the transformation of photoenergy in algae differed from cell proliferation and algal biomass, which was impacted by the different P regimes. Therefore, three indicators, including OD, Chl *a*, and yield, were utilized to investigate algal toxicity under the different P forms associated with As(V) as discussed below.

3.2. Arsenate toxicity

96-h EC₅₀ values of As(V) toxicity in *M. aeruginosa* under the different P treatments were found to be well fitted using a sigmoidal dose-response curve with an R^2 range from 0.780 to 0.979 (Table 2). From ANOVA results of OD, Chl *a*, and yield, the no-observed-effect concentration (NOEC) and the lowest-observed-effect concentration (LOEC) of As(V) were similar under the different DOP treatments (i.e., βP , ATP, and GP) with a NOEC of

Table 1

Pearson correlation coefficient between chlorophyll *a* (Chl *a*) and optical density (OD) with yield under the different phosphorus regimes ($n = 21$); IP: inorganic phosphate, βP : β -sodium glycerophosphate, ATP: adenosine 5'-triphosphate, GP: D-Glucose-6-phosphate disodium.

	yield	IP	βP	ATP	GP
Chl <i>a</i>		-0.202	-0.601**	-0.864**	-0.845**
OD		-0.434*	-0.662**	-0.599**	-0.614**

* $P < 0.05$, ** $P < 0.01$.

Table 2

Arsenate 96-h EC₅₀ values for *Microcystis aeruginosa* obtained from optical density (OD), chlorophyll *a* (Chl *a*), and yield under the different phosphorus regimes by fitting with a sigmoidal concentration–response curve ($\mu\text{g}\cdot\text{L}^{-1}$); IP: inorganic phosphate, βP : β -sodium glycerophosphate, ATP: adenosine 5'-triphosphate, GP: D-Glucose-6-phosphate disodium.

	IP	βP	ATP	GP
OD	5.08×10^9	4.28×10^4	4.02×10^4	5.80×10^5
R ²	0.974	0.975	0.919	0.951
Chl <i>a</i>	1.60×10^9	5.70×10^4	4.67×10^4	6.88×10^5
R ²	0.979	0.964	0.929	0.920
yield	3.11×10^6	2.57×10^5	5.58×10^4	8.92×10^5
R ²	0.916	0.925	0.896	0.780

10^4 $\mu\text{g}/\text{L}$ and a LOEC of 10^5 $\mu\text{g}/\text{L}$. Meanwhile, the two NOEC and LOEC values were lower under DOP treatments than under the IP treatment (10^5 and 10^6 $\mu\text{g}/\text{L}$, respectively). These results indicated that As(V) toxicity of *M. aeruginosa* was virtually unaffected by the different DOP forms at a comparable As level in water, but it was significantly different between DOP and IP. Specifically, IP could significantly alleviate As(V) stress on *M. aeruginosa* due to its unique ability in identifying IP and As(V) (Wang et al., 2014).

Furthermore, significant differences were found between the 96-h EC₅₀ values obtained from OD, Chl *a*, and yield ($P < 0.05$), and the species' tolerance to As(V) under the different P treatments followed the order IP > GP > βP > ATP (Table 2). Compared to the DOP treatments, the higher As(V) tolerance under the IP treatment could be attributable to the similar chemical structures between two ionic compounds (PO_4^{3-} and AsO_4^{3-}), which resulted in an overall better IP and As(V) discrimination of *M. aeruginosa* (Wang et al., 2013; Wang et al., 2014). This confirmed that *M. aeruginosa* had different P uptake mechanisms for the given DOP sources compared to IP, which caused As(V) to have an additional impact on algal growth. The 96-h EC₅₀ concentrations of As(V) under the IP treatment followed in descending order: OD > Chl *a* > yield. Under the different DOP treatments, however, the order was yield > Chl *a* > OD. These results indicated that As(V) toxicity of *M. aeruginosa* was affected by the different forms of P, including DOP and IP.

3.3. Quantifying mRNA by Real-Time PCR

The two As genes (*arsC* and *arsM*) are critical in understanding As bioreduction and methylation processes in algae. The relative gene expression levels ($2^{-\Delta\text{CT}}$) of *arsC* were higher under the DOP treatments than the IP treatment, which specifically followed the order GP > ATP > βP > IP (Fig. 1a). Similarly, the relative gene expression levels of *arsM* were higher under the DOP treatments than the IP treatment, wherein the relative gene expression levels under the different organic P forms were not significant (Fig. 1b). Furthermore, the gene expression of P transport as it pertains to these genes is helpful in understanding the combined roles of P and As(V) in algae under different P forms. For NIES-843-1, significant differences were found between the DOP and IP treatments, followed by ATP > GP ~ βP > IP (Fig. 1c). Similarly, significant differences in NIES-843-2 were found between the DOP and IP treatments (GP ~ βP ~ ATP > IP) (Fig. 1d). The differences between the four As and P functional genes under the different P treatments could potentially provide information on how As biotransformation and bioaccumulation are impacted by the different P forms, which is discussed below.

3.4. Arsenic uptake and biotransformation

3.4.1. Changes in arsenic species in media

In media, differences in TAs under the different P treatments

were not significant (Fig. 2). Specifically, As(V) remained the predominant species, accounting for greater than 94.0% of TAs under the IP, βP , and ATP treatments. This was followed by DMA, which ranged from 1.81% to 5.10% and As(III), less than 1.00% of TAs. In the GP treatment media, As(III) accounted for 39.2% of TAs while As(V) accounted for 56.4% of TAs, indicating that As(III) content was second to the dominant presence of As(V) in the GP media. This demonstrated that the reduction of As(V) in *M. aeruginosa* was greatly accelerated in the presence of GP. The presence of a large amount of As(III) in GP media could potentially strengthen the ecological risks of As and must therefore be taken into account. Moreover, MMA was also identified in IP and GP media. Compared to the IP medium, relatively higher DMA concentrations were found in all three DOP media ($P < 0.05$). This indicated that As methylation of *M. aeruginosa* was promoted under DOP conditions.

3.4.2. Arsenic speciation in algal cells

Compared to the DOP treatments, the IP treatment had the minimum intracellular TAs content (22.8 ± 1.71 $\mu\text{g}/\text{g}$; Fig. 3), corresponding to the maximum As(V) EC₅₀ value (Table 2), demonstrating that *M. aeruginosa* can discriminate between IP and As(V) (Wang et al., 2013). Furthermore, DOP can greatly facilitate the accumulation of As, particularly βP , supported by the higher intracellular TAs content under βP conditions (Fig. 3).

Additionally, compared to the IP treatment, higher As(III) contents were found in algal cells under the DOP treatments ($P < 0.05$; Fig. 3), particularly the GP treatment. Specifically, GP supported the production of As(III), subsequently exceeding As(V) as the main As species in *M. aeruginosa* (Fig. 3). This implied that DOP promotes the bioreduction of As(V) to As(III), especially under GP conditions. Meanwhile, trace amounts of DMA were detected in algal cells under the GP, ATP, and IP treatments, and MMA was only found under GP conditions. Interestingly, DMA was not found in algal cells under the βP treatment, but it was present in the medium. A potential explanation for this is that DMA produced in algae was released so rapidly that its concentrations were lower than the detection limit (Yan et al., 2014). Therefore, taken together with the observations of As species in algal cells and media, the DOP forms were demonstrated to be able to enhance As(V) bioreduction and subsequently methylation in this algae species. In particular, compared to the other P forms, the higher As(III) and MMA found in both algal cells and media under GP treatment conditions verified that As(V) reduction and the subsequent As(III) methylation were greatly facilitated in *M. aeruginosa* by the presence of this DOP form. Therefore, *M. aeruginosa* can promote As(V) detoxification as the precursor of the crucial steps involved in As methylation (Hellweger and Lall, 2004).

3.5. Changes in phosphorus forms

The identification of P uptake by *M. aeruginosa* under the different P treatments involved the investigation of TP and IP in media and intracellular TP content as well as the ratio of P/As (TP: TAs) in algal cells under the different P treatments following 10 d in algal culture media (Fig. 4). Compared to the IP treatment, higher TP concentrations were found in media under the DOP treatments. In contrast, IP content in media followed the order ATP > βP ~ IP > GP (Fig. 4a), illustrating the various faculties *M. aeruginosa* has in converting the different forms of DOP (i.e., ATP, βP , and GP) to IP. Specifically, the transformation rate of these three different DOP forms into IP was in the order ATP > GP > βP (Table S2), assessed using a linear kinetic model. Previous studies verified the ability of *M. aeruginosa* to transform DOP to IP through continuous alkaline phosphatase (ALP) hydrolysis, which improves DOP utilization (Li et al., 2015). However, some studies reported that the metabolism

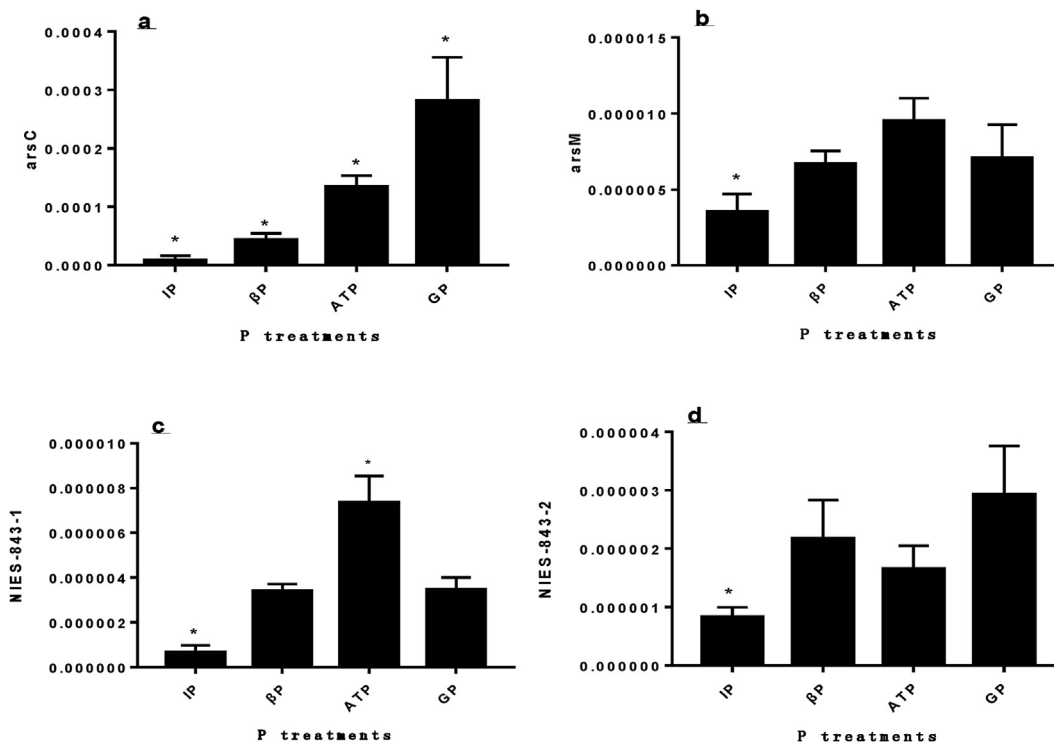


Fig. 1. Relative expression levels ($2^{-\Delta CT}$) of the four functional genes at 12 h exposure. (a): *arsM*, (b): *arsC*, (c): NIES-843-1 (5862636), and (d): NIES-843-2 (5866103). * Denotes significant differences among the different P treatments at $P < 0.05$. IP: inorganic phosphate, βP: β-sodium glycerophosphate, ATP: adenosine 5'-triphosphate, GP: D-Glucose-6-phosphate disodium.

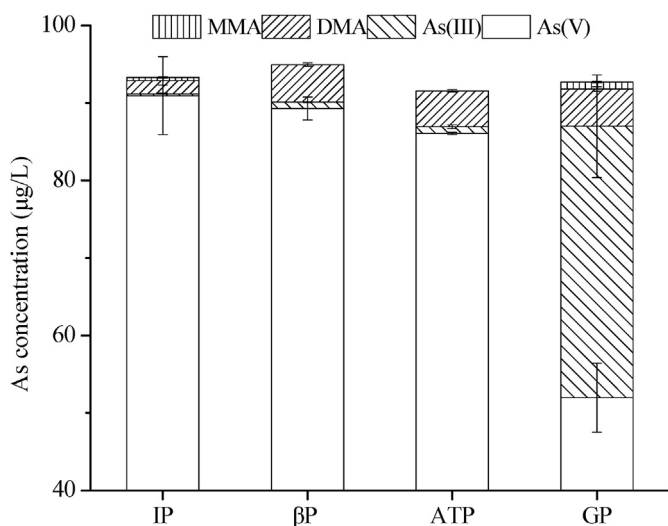


Fig. 2. Different arsenic species content in media under the different phosphorus treatments; IP: inorganic phosphate, βP: β-sodium glycerophosphate, ATP: adenosine 5'-triphosphate, GP: D-Glucose-6-phosphate disodium.

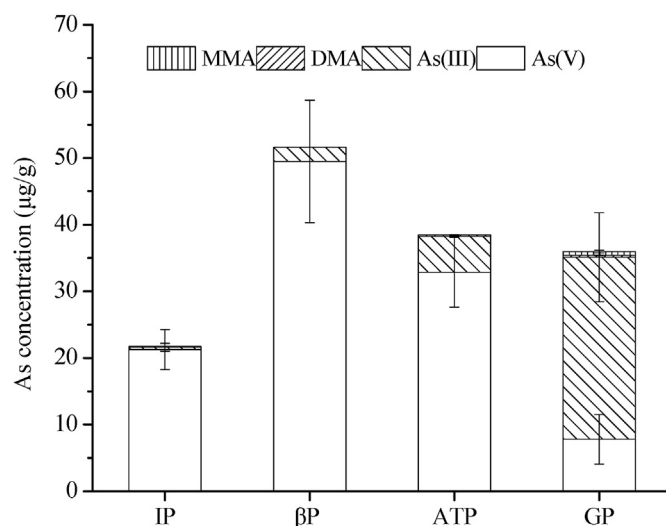


Fig. 3. Different arsenic speciation in algal cells under the different phosphorus treatments after 10 d exposure in culture media; IP: inorganic phosphate, βP: β-sodium glycerophosphate, ATP: adenosine 5'-triphosphate, GP: D-Glucose-6-phosphate disodium.

of DOP in algae was not regulated by ALP (Huang et al., 2005). In our study, the transformation rate of GP to IP was higher than that of βP, which was not regulated by ALP. For instance, Ren et al. (2017) demonstrated that the production of ALP under GP conditions was slightly lower than that under βP conditions for *M. aeruginosa*. Due to the absence of evidence associated with the direct adsorption of DOP and its subsequent utilization in algal cells, the transformation and metabolic mechanisms of DOP for *M. aeruginosa* remain unclear and therefore requires further study.

Furthermore, intracellular TP content in *M. aeruginosa* ranged from 1.58 to 3.41 mg/g under the different P treatments, following the order IP > βP ~ ATP > GP (Fig. 4b). Moreover, higher intracellular TP content in *M. aeruginosa* corresponded to higher intracellular TAs under the different DOP treatments. This corresponding sequence illustrated that *M. aeruginosa* could not discriminate As(V) under different DOP environments. Additionally, the maximum value of the intracellular P/As ratios under the IP

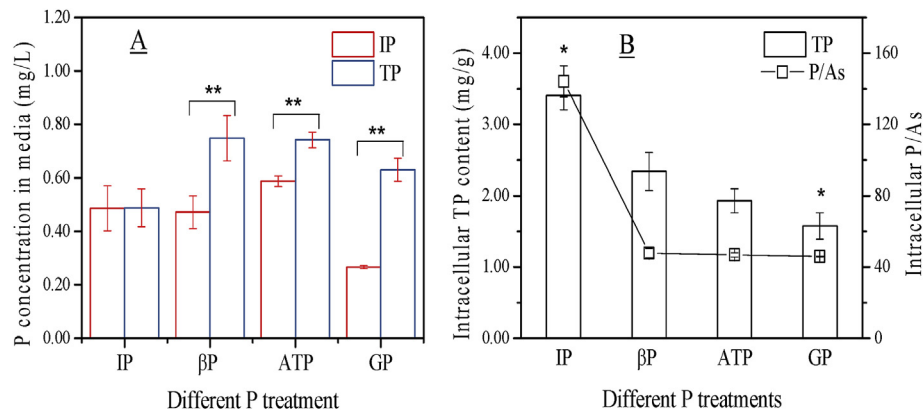


Fig. 4. Total phosphorus (TP) and inorganic phosphate (IP) content in (A) media and intracellular TP content as well as (B) the P/As ratio in *Microcystis aeruginosa* under the different phosphorus treatments after 10 d exposure in culture media; ** Denotes significant differences among the inner P treatments at $P < 0.05$; * Denotes significant differences among different P treatments at $P < 0.05$. IP: inorganic phosphate, β P: β -sodium glycerophosphate, ATP: adenosine 5'-triphosphate, GP: D-Glucose-6-phosphate disodium.

treatment further confirmed that *M. aeruginosa* could discriminate between As(V) and IP. This was due to competitive transporters between phosphate and As(V) in algal cells. Similar results were confirmed for *Pteris vittata* (Wang et al., 2002) and *Pennisetum clandestinum* (Panuccio et al., 2012). In contrast, the higher TP content in media combined with the lower intracellular TP content under the different DOP treatments further confirmed the difficulty that *M. aeruginosa* has in their utilization compared to the IP treatment. Consequently, the relative gene expressions of the two P transport functional genes were higher under the DOP treatments compared to the IP treatment, which could stimulate *M. aeruginosa* and allow for the required amount of P necessary to support growth. Other studies reported similar findings; namely, *M. aeruginosa* could rapidly store IP as polyphosphates in cells (Chrost and Overbeck, 1987) and hydrolyze DOP to IP by means of cellular surface enzymes for direct utilization or transient accumulation (Li et al., 2015; Ren et al., 2017). Additionally, the P/As ratio in algal cells under the IP treatment was greater by a factor of three compared to that under the DOP treatments. Furthermore, no significant differences were observed among these DOP treatments. The similar P/As ratio in algal cells under the different DOP treatments (Fig. 4b) implied that As(V) uptake and bioaccumulation were positively correlated to the way in which the different DOP forms were utilized in *M. aeruginosa* owing to the fact that there were some differences in TP and IP in culture media as well as intracellular TP under the different DOP treatments. Therefore, the way in which As(V) uptake and bioaccumulation take place in *M. aeruginosa* are impacted not only by the differences between the inorganic and organic P forms but also by the differences among the DOP forms.

3.6. Subcellular distribution of arsenic and phosphorus

All observations made of subcellular fractions indicated that the different P treatments primarily affected the subcellular distribution of P in *M. aeruginosa* ($P < 0.05$; Fig. S2). Moreover, P was found to primarily distribute HSP within algal cells of *M. aeruginosa* (at approximately 57.6%–71.2% TP) with significant differences observed among the different P treatments ($P < 0.05$; Fig. S2). Previously, it was demonstrated that P primarily resided in cytoplasmic supernatant fractions, including MRG, organelles, and HSP in *Pteris vittata* L. (Chen et al., 2005). Similarly, in this study P was primarily distributed in cytoplasmic supernatant fractions, including metal-sensitive fractions (MSF, organelles and HSP). This indicated the important role that P plays in supporting

M. aeruginosa growth as well as its level of tolerance given its ability to discriminate between As(V) and IP. Specifically, P content in cellular debris was second only to HSP under the DOP treatments, while HDP had the second highest distribution fraction under the IP treatment (Fig. S2). Despite the fact that the different DOP forms used in this study comprised of three different macromolecules, all three DOP forms could possess similar P transporters in cells to promote their absorption, which would not result in a significant difference of P accumulation in cell debris (Fig. 5). For the GP treatment, P distribution in HDP was lowest compared to the other P treatments (6.91 μ g/g), and P distribution in organelles was greater by an approximate factor of nine compared to the β P and ATP treatments. Compared to the β P and ATP treatments, the higher P distribution in MSF (including organelles and HSP) could have potentially led to a significant decrease in As(V) toxicity under the GP treatment (Fig. 5; Fig. S2; Table 2). Similarly, the higher P distribution in MSF in the IP treatment confirmed that *M. aeruginosa* underwent lower toxic stress (i.e., higher 96-h EC_{50} values; Table 2) compared to the DOP treatments.

Furthermore, there were significant differences in As subcellular distribution between the IP treatment and the different DOP treatments, especially for As content in cellular debris (Fig. 5; Fig. S3). For the IP treatment, As was found to be largely distributed in HDP, organelles, and HSP, accounting for approximately 40.8%, 22.0%, and 20.9% of TAs, respectively. In contrast, for the different DOP treatments, As was mainly distributed in cellular debris, accounting for greater than 70% of TAs, for which HDP only accounted for 2% of TAs (Fig. S3). This implied that these DOP forms promoted the distribution of As in cellular debris, which could preclude As(V) from entering algal cells, subsequently reducing toxic stress. Additionally, significant differences in As distribution in MRG, organelles, and HSP were observed among the different P treatments ($P < 0.05$). This showed that the different P treatments mainly affected As distribution in the cytoplasmic fraction of the supernatant, including MRG, organelles, and HSP (Chen et al., 2005). Furthermore, given the fact that differences in As subcellular distribution among the three different DOP treatments were not significant, As(V) distribution in *M. aeruginosa* could potentially be the same as the different DOP treatments while being different from the IP treatment.

Previous studies demonstrated that the subcellular distribution of metals reflects their internal processes during metal accumulation, which potentially supports a specific explanation pertaining to metal toxicity and tolerance (Jenkins and Mason, 1988; Klerks and Bartholomew, 1991; Li et al., 2016). Additionally, metals associated

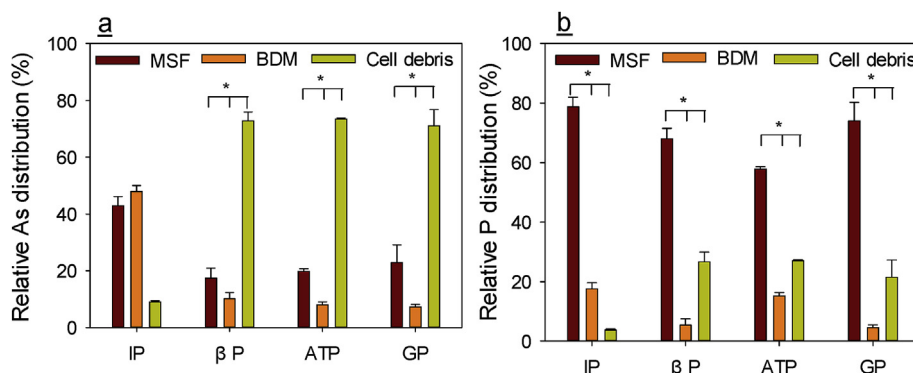


Fig. 5. Relative subcellular distribution (%) of arsenic (a) and phosphorus (b) in *Microcystis aeruginosa* after 10 d exposure to 100 ppb As(V) under the different phosphorus treatments. metal-sensitive fractions (MSF): organelles and heat-stable proteins (HSP); biologically detoxified fractions (BDM): metal-rich granules (MRG) and heat-denatured proteins (HDP). * Denotes significant differences among distributions for the inner group at $P < 0.05$; IP: inorganic phosphate, βP: β-sodium glycerophosphate, ATP: adenosine 5'-triphosphate, GP: D-Glucose-6-phosphate disodium.

with organelles and HSP were collectively viewed as MSF (Jenkins and Mason, 1988; Wallace et al., 2000), while MRG and HDP were collectively viewed as biologically detoxified fractions (BDM), which provides metal tolerance and perhaps resistance (Li et al., 2011; Luo et al., 2018). In this study, there were not significant differences between MSF and BDM under the IP treatment. Furthermore, compared to BDM, the higher MSF distribution of As in *M. aeruginosa* under the different DOP treatments could explain the higher toxicity of As(V) with lower 96-h EC_{50} values (Fig. 5).

3.7. Environmental implications

In this study, As(V) bioreduction and its subsequent methylation were found to differ to some extent in *M. aeruginosa*, and this was due to its different DOP uptake and transformation processes, algal discrimination between P and As(V), and the physiological response of algae under different P conditions. Obviously, *M. aeruginosa* can utilize βP, ATP, and GP to sustain algal growth. Moreover, it exhibited similar characteristics, namely, an increase in cell number and Chl *a* and a decrease in yield under the three different DOP treatments. Compared to the IP treatment, the results showed the higher TP content observed in media combined with the lower intracellular TP content under the different DOP treatments, which demonstrated the difficulty that *M. aeruginosa* has in utilizing DOP. Consequently, the relative expressions of the two P transport functional genes were greater under the DOP treatments than under the IP treatment, which could help *M. aeruginosa* in obtaining the P necessary to support algal growth. Higher P content typically results in lower instances of intracellular As in algae due to its discrimination between IP and As(V). Accordingly, the higher P distribution in MSF found under the IP treatment could potentially be the result of lower toxic stress (i.e., higher 96-h EC_{50} values; Table 2) compared to the DOP treatments. Moreover, the higher P distribution in the MSF resulted in a more significant decrease in As(V) toxicity under the GP treatment compared to the βP and ATP treatments. Similarly, the higher As distribution found in the MSF of *M. aeruginosa* under the different DOP treatments also confirmed higher toxicity of As(V) with lower 96-h EC_{50} values.

Collectively, our findings confirmed the existence of an underlying mechanism of As(V) accumulation and methylation in *M. aeruginosa* that was enhanced by the different DOP forms. Specifically, *M. aeruginosa* is able to discriminate between As(V) and IP with the result that lower IP promotes higher intracellular As accumulation in algae. However, this particular algae is unable to discriminate between As(V) and DOP, a conclusion that was partly

supported by the higher intracellular TP content along with the higher intracellular TAs under the different DOP treatments. Additionally, the transformation rate of βP into phosphate was lower than that of ATP and GP in media. The result of this could be lower IP in media at the start of As uptake in *M. aeruginosa* according to their lowest IP transformation rate (Table S2) under the βP treatment. Collectively, As accumulation in algal cells can be greatly enhanced under DOP treatments, particularly βP. Furthermore, As(V) reduction and subsequent As(III) methylation were greatly facilitated by DOP in *M. aeruginosa*, which was confirmed by the higher relative gene expression of the two functional genes (*arsC* and *arsM*). This could have been caused by an increase of algal stress under the DOP treatments, subsequently promoting As(V) biotransformation under these DOP conditions. Additionally, more attention must be paid to As(III) abundance in both algal cells and media in the presence of GP given that it is more toxic than As(V). Reducing As(V) content under GP conditions in water bodies is critical. This will decrease the ecological risk of As(V), particularly when As contamination and higher GP levels coexist.

The findings from this study provide new insight into promoting As(V) bioremediation, especially for microalgae under controlled P conditions. Specifically, DOP forms can be utilized to enhance As accumulation in *M. aeruginosa*, particularly βP. In contrast, DOP forms can be utilized to facilitate As(V) reduction and subsequent As(III) methylation using this alga species, particularly GP. Results from this study will also help in our understanding of the toxic effects and mechanisms of As(V) on cyanobacteria under different P conditions.

4. Conclusions

In this study, the subcellular distribution of P and As can be used to verify As toxicity in algae. Specifically, the higher P distribution in the MSF under the IP treatment could potentially derive from the lower toxic stress of *M. aeruginosa* compared to the DOP treatments. Meanwhile, the higher As distribution in the MSF of *M. aeruginosa* under the DOP treatments could have resulted from its higher toxic stress with lower 96-h EC_{50} values. Furthermore, the inability to discriminate between DOP and As(V) enhanced As bioaccumulation in *M. aeruginosa*, especially under the βP treatment, which resulted from its lower IP transformation rate. As(V) reduction and its subsequent methylation were also accelerated under the DOP treatments, especially GP. A large amount of As(III) was thus found in both media and cells, heightening the overall ecological risk under the GP treatment. More research is needed to

understand the complexity as it relates to the physiological response of algae and DOP uptake as well as its transformation within algal cells.

Declarations of interest

None.

Acknowledgements

We would like to thank Brian Doonan for his language help in writing this paper. This study was financially supported by the Natural Science Foundation of China (Project Nos. 41401552, 41271484, and 41773100), the Natural Science Foundation of Fujian Province (2016J01691 and 2017Y0081), and Program for New Century Excellent Talents in Fujian Province University.

Appendix A. Supplementary data

Supplementary data to this article can be found online at <https://doi.org/10.1016/j.envpol.2019.06.126>.

References

- Bengt Boström, G.P., Broberg, Brita, 1988. Bioavailability of different phosphorus forms in freshwater. *Hydrobiologia* 133–155.
- Björkman, K.M., Karl, D.M., 2003. Bioavailability of dissolved organic phosphorus in the euphotic zone at station ALOHA, North Pacific subtropical Gyre. *Limnol. Oceanogr.* 48, 1049–1057.
- Chalifour, A., Juneau, P., 2011. Temperature-dependent sensitivity of growth and photosynthesis of *Senedesmus obliquus*, *Navicula pelliculosa* and two strains of *Microcystis aeruginosa* to the herbicide atrazine. *Aquat. Toxicol.* 103, 9–17.
- Chen, J., Yoshinaga, M., Garbinski, L.D., Rosen, B.P., 2016. Synergistic interaction of glyceraldehydes-3-phosphate dehydrogenase and ArsJ, a novel organoarsenical efflux permease, confers arsenate resistance. *Mol. Microbiol.* 100, 945–953.
- Chen, T.B., Yan, X.L., Liao, X.Y., Xiao, X.Y., Huang, Z.C., Xie, H., Zhai, L.M., 2005. Subcellular distribution and compartmentalization of arsenic in *Pteris vittata* L. *Chin. Sci. Bull.* 50, 2843–2849.
- Chrost, R.J., Overbeck, J., 1987. Kinetics of alkaline-phosphatase activity and phosphorus availability for phytoplankton and bacterioplankton in lake plussee (North-German eutrophic lake). *Microb. Ecol.* 13, 229–248.
- Davis, T.W., Bullerjahn, G.S., Tuttle, T., McKay, R.M., Watson, S.B., 2015. Effects of increasing nitrogen and phosphorus concentrations on phytoplankton community growth and toxicity during planktothrix blooms in Sandusky Bay, lake Erie. *Environ. Sci. Technol.* 49, 7197–7207.
- Elias, M., Wellner, A., Goldin-Azulay, K., Chabriere, E., Vorholt, J.A., Erb, T.J., Tawfik, D.S., 2012. The molecular basis of phosphate discrimination in arsenate-rich environments. *Nature* 491, 134–137.
- Fu, F.X., Zhang, Y.H., Feng, Y.Y., Hutchins, D.A., 2006. Phosphate and ATP uptake and growth kinetics in axenic cultures of the cyanobacterium *Synechococcus* CCMF 1334. *Eur. J. Phycol.* 41, 15–28.
- Harke, M.J., Berry, D.L., Ammerman, J.W., Gobler, C.J., 2012. Molecular response of the bloom-forming cyanobacterium, *Microcystis aeruginosa*, to phosphorus limitation. *Microb. Ecol.* 63, 188–198.
- Haygarth, P.M., Wood, F.L., Heathwaite, A.L., Butler, P.J., 2005. Phosphorus dynamics observed through increasing scales in a nested headwater-to-river channel study. *Sci. Total Environ.* 344, 83–106.
- Hellweger, F., Lall, U., 2004. Modeling the effect of algal dynamics on arsenic speciation in lake biwa. *Environ. Sci. Technol.* 38, 6716–6723.
- Huang, B., Ou, L., Hong, H., Luo, H., Wang, D., 2005. Bioavailability of dissolved organic phosphorus compounds to typical harmful dinoflagellate *Prorocentrum donghaiense* Lu. *Mar. Pollut. Bull.* 51, 838–844.
- Hudson, J.J., Taylor, W.D., Schindler, D.W., 2000. Phosphate concentrations in lakes. *Nature* 406, 54–56.
- Hughes, M.F., Beck, B.D., Chen, Y., Lewis, A.S., Thomas, D.J., 2011. Arsenic exposure and toxicology: a historical perspective. *Toxicol. Sci.* 123, 305–332.
- Jenkins, K.D., Mason, A.Z., 1988. Relationships between subcellular distributions of cadmium and perturbations in reproduction in the polychaete *Neanthes-arenaceodentata*. *Aquat. Toxicol.* 12, 229–244.
- Kaneko, T., Nakajima, N., Okamoto, S., Suzuki, I., Tanabe, Y., Tamaoki, M., Nakamura, Y., Kasai, F., Watanabe, A., Kawashima, K., Kishida, Y., Ono, A., Shimizu, Y., Takahashi, C., Minami, C., Fujishiro, T., Kohara, M., Katoh, M., Nakazaki, N., Nakayama, S., Yamada, M., Tabata, S., Watanabe, M.M., 2007. Complete genomic structure of the bloom-forming toxic cyanobacterium *Microcystis aeruginosa* NIES-843. *DNA Res.* 14, 247–256.
- Karadjova, I.B., Slaveykov, V.I., Tsalev, D.L., 2008. The biouptake and toxicity of arsenic species on the green microalga *Chlorella salina* in seawater. *Aquat. Toxicol.* 87, 264–271.
- Karl, D.M., Björkman, K.M., 2001. Phosphorus Cycle in Seawater: Dissolved and Particulate Pool Inventories and Selected Phosphorus Fluxes. *Methods in Microbiology*. Academic Press, pp. 239–270.
- Klerks, P.L., Bartholomew, P.R., 1991. Cadmium accumulation and detoxification in a Cd-resistant population of the Oligochaete *limnodrilus-hoffmeisteri*. *Aquat. Toxicol.* 19, 97–112.
- Lei, M., Wan, X.M., Huang, Z.C., Chen, T.B., Li, X.W., Liu, Y.R., 2012. First evidence on different transportation modes of arsenic and phosphorus in arsenic hyper-accumulator *Pteris vittata*. *Environ. Pollut.* 161, 1–7.
- Lessl, J.T., Ma, L.Q., 2013. Sparingly-soluble phosphate rock induced significant plant growth and arsenic uptake by *Pteris vittata* from three contaminated soils. *Environ. Sci. Technol.* 47, 5311–5318.
- Levy, J., Stauber, J.L., Adams, M.S., Maher, W.A., Kirby, J.K., Jolley, D.F., 2005. Toxicity, biotransformation, and mode of action of arsenic in two freshwater microalgae (*Chlorella* sp. and *Monoraphidium arcuatum*). *Environ. Toxicol. Chem.* 24, 2630–2639.
- Li, B., Brett, M.T., 2013. The influence of dissolved phosphorus molecular form on recalcitrance and bioavailability. *Environ. Pollut.* 182, 37–44.
- Li, D.D., Zhou, D.M., Wang, P., Weng, N.Y., Zhu, X.D., 2011. Subcellular Cd distribution and its correlation with antioxidant enzymatic activities in wheat (*Triticum aestivum*) roots. *Ecotoxicol. Environ. Saf.* 74, 874–881.
- Li, J., Wang, Z., Cao, X., Wang, Z., Zheng, Z., 2015. Effect of orthophosphate and bioavailability of dissolved organic phosphorus compounds to typically harmful cyanobacterium *Microcystis aeruginosa*. *Mar. Pollut. Bull.* 92, 52–58.
- Li, M., Luo, Z., Yan, Y., Wang, Z., Chi, Q., Yan, C., Xing, B., 2016. Arsenate accumulation, distribution, and toxicity associated with titanium dioxide nanoparticles in *Daphnia magna*. *Environ. Sci. Technol.* 50, 9636–9643.
- Lippemeier, S., Frampton, D.M.F., Blackburn, S.I., Geier, S.C., Negri, A.P., 2003. Influence of phosphorus limitation on toxicity and photosynthesis of *Alexandrium minutum* (Dinophyceae) monitored by in-line detection of variable chlorophyll fluorescence. *J. Phycol.* 39, 320–331.
- Luo, Z., Li, M., Wang, Z., Li, J., Guo, J., Rosenfeldt, R.R., Seitz, F., Yan, C., 2018. Effect of titanium dioxide nanoparticles on the accumulation and distribution of arsenate in *Daphnia magna* in the presence of an algal food. *Environ. Sci. Pollut. Res. Int.* 25, 20911–20919.
- Mandal, B.K., Suzuki, K.T., 2002. Arsenic round the world: a review. *Talanta* 58, 201–235.
- Markley, C.T., Herbert, B.E., 2010. Modeling phosphate influence on arsenate reduction kinetics by a freshwater cyanobacterium. *Environ. Model. Assess.* 15, 361–368.
- Miao, A.J., Wang, N.X., Yang, L.Y., Wang, W.X., 2012. Accumulation kinetics of arsenic in *Daphnia magna* under different phosphorus and food density regimes. *Environ. Toxicol. Chem.* 31, 1283–1291.
- Monbet, P., McKelvie, I.D., Saefumillah, A., Worsfold, P.J., 2007. A protocol to assess the enzymatic release of dissolved organic phosphorus species in waters under environmentally relevant conditions. *Environ. Sci. Technol.* 41, 7479–7485.
- Monbet, P., McKelvie, I.D., Worsfold, P.J., 2009. Dissolved organic phosphorus speciation in the waters of the Tamar estuary (SW England). *Geochim. Cosmochim. Acta* 73, 1027–1038.
- Orchard, E.D., Ammerman, J.W., Lomas, M.W., Dyrman, S.T., 2010. Dissolved inorganic and organic phosphorus uptake in *Trichodesmium* and the microbial community: the importance of phosphorus ester in the Sargasso Sea. *Limnol. Oceanogr.* 55, 1390–1399.
- Oremland, R.S., Stolz, J.F., 2003. The ecology of arsenic. *Science* 300, 939–944.
- Panuccio, M.R., Logoteta, B., Beone, G.M., Cagnin, M., Cacco, G., 2012. Arsenic uptake and speciation and the effects of phosphate nutrition in hydroponically grown kikuyu grass (*Pennisetum clandestinum* Hochst). *Environ. Sci. Pollut. Control Ser.* 19, 3046–3053.
- Qin, C., Liu, H., Liu, L., Smith, S., Sedlak, D.L., Gu, A.Z., 2015. Bioavailability and characterization of dissolved organic nitrogen and dissolved organic phosphorus in wastewater effluents. *Sci. Total Environ.* 511, 47–53.
- Rahman, M.A., Hasegawa, H., Lim, R.P., 2012. Bioaccumulation, biotransformation and trophic transfer of arsenic in the aquatic food chain. *Environ. Res.* 116, 118–135.
- Rahman, S., Kim, K.H., Saha, S.K., Swaraz, A.M., Paul, D.K., 2014. Review of remediation techniques for arsenic (As) contamination: a novel approach utilizing bio-organisms. *J. Environ. Manag.* 134C, 175–185.
- Ren, L., Wang, P., Wang, C., Chen, J., Hou, J., Qian, J., 2017. Algal growth and utilization of phosphorus studied by combined mono-culture and co-culture experiments. *Environ. Pollut.* 220, 274–285.
- Secco, D., Jabnoute, M., Walker, H., Shou, H., Wu, P., Poirier, Y., Whelan, J., 2013. Spatio-temporal transcript profiling of rice roots and shoots in response to phosphate starvation and recovery. *Plant Cell* 25, 4285–4304.
- Wallace, W.G., Brouwer, T.M.H., Brouwer, M., Lopez, G.R., 2000. Alterations in prey capture and induction of metallothioneins in grass shrimp fed cadmium-contaminated prey. *Environ. Toxicol. Chem.* 19, 962–971.
- Wang, C., He, R., Wu, Y., Lurling, M., Cai, H., Jiang, H.L., Liu, X., 2017a. Bioavailable phosphorus (P) reduction is less than mobile P immobilization in lake sediment for eutrophication control by inactivating agents. *Water Res.* 109, 196–206.
- Wang, J.Z., Meharg, F.J., Raab, A.A., Feldmann, A., McGrath, J., S. P., 2002. Mechanisms of arsenic hyperaccumulation in *Pteris vittata*. Uptake kinetics, interactions with phosphate, and arsenic speciation. *Plant Physiol.* 130, 1552–1561.
- Wang, N.X., Li, Y., Deng, X.H., Miao, A.J., Ji, R., Yang, L.Y., 2013. Toxicity and bioaccumulation kinetics of arsenate in two freshwater green algae under different

- phosphate regimes. *Water Res.* 47, 2497–2506.
- Wang, Y., Zhang, C.H., Lin, M.M., Ge, Y., 2016. A symbiotic bacterium differentially influences arsenate absorption and transformation in *Dunaliella salina* under different phosphate regimes. *J. Hazard Mater.* 318, 443–451.
- Wang, Z., Luo, Z., Yan, C., Rosenfeldt, R.R., Seitz, F., Gui, H., 2018. Biokinetics of arsenate accumulation and release in *Microcystis aeruginosa* regulated by common environmental factors: practical implications for enhanced bioremediation. *J. Clean. Prod.* 199, 112–120.
- Wang, Z.H., Luo, Z.X., Yan, C.Z., Che, F.F., Yan, Y.M., 2014. Arsenic uptake and depuration kinetics in *Microcystis aeruginosa* under different phosphate regimes. *J. Hazard Mater.* 276, 393–399.
- Wang, Z.H., Luo, Z.X., Yan, C.Z., Xing, B.S., 2017b. Impacts of environmental factors on arsenate biotransformation and release in *Microcystis aeruginosa* using the Taguchi experimental design approach. *Water Res.* 118, 167–176.
- Whitton, B.A., Grainger, S.L., Hawley, G.R., Simon, J.W., 1991. Cell-bound and extracellular phosphatase activities of cyanobacterial isolates. *Microb. Ecol.* 21, 85–98.
- Worsfold, P., McKelvie, I., Monbet, P., 2016. Determination of phosphorus in natural waters: a historical review. *Anal. Chim. Acta* 918, 8–20.
- Wu, J., Sunda, W., Boyle, E.A., Karl, D.M., 2000. Phosphate depletion in the western North Atlantic ocean. *Science* 289, 759–762.
- Xu, J.Y., Li, H.B., Liang, S., Luo, J., Ma, L.N.Q., 2014. Arsenic enhanced plant growth and altered rhizosphere Characteristics of hyperaccumulator *Pteris vittata*. *Environ. Pollut.* 194, 105–111.
- Yan, C., Wang, Z., Luo, Z., 2014. Arsenic efflux from *Microcystis aeruginosa* under different phosphate regimes. *PLoS One* 9, e116099.
- Zhang, S., Rensing, C., Zhu, Y.G., 2014. Cyanobacteria-mediated arsenic redox dynamics is regulated by phosphate in aquatic environments. *Environ. Sci. Technol.* 48, 994–1000.